# Layout of cross braces on progressive collapse analysis of a 3D 12-story steel composite frame structures

Yi Hu* and Junhai Zhao**,*

*School of Civil Engineering, Central South University of Forestry and Technology, Changsha 410004, China*
**School of Civil Engineering, Chang'an University, Xi'an 710061, China*
*Corresponding Author: zhaojh@chd.edu.cn*

## ABSTRACT

In this paper, cross braces are provided to mitigate the dynamic responses of steel frames caused by column-remove scenarios. To evaluate the effectiveness of cross braces with different layout on enhancing the progressive collapse resisting capacity of the structures, alternative path method (APM) is performed on structural nonlinear dynamic history analysis. Firstly, a three-dimensional finite element model for 12-story steel composite frame structure is built with considering the contribution of the composite behavior of the floor system. Then, the FEM modeling method is verified by a progressive collapse test. Finally, a series of progressive collapse analyses on such model with different column-remove scenarios and layout of cross braces are carried out. The results show that the cross braces could mitigate the dynamic response caused by column failure in the affected bay, but no obvious mitigation were observed in the other bays. Cross braces blocked the horizontal development of structural progressive collapse for the structure with vertical layout of cross braces (SF-VB), which might aggravate the dynamic response of the affected bay through protecting the residual structure. Cross braces layout at the top layer (TB) decreased the peak displacement of corner column failure mode above 50% and was about 30% for the side column failure mode. The dynamic increase factor (DIF) of the most models was about 1.5, which demonstrated that the value given by the standards might result with some conservatism, but the DIF might be close to the given value for SF-VB. Such results provided basis for information for progressive collapse prevention designs of such structural systems.

**Keywords:** Progressive collapse; Steel frame; Cross brace; Layout; Dynamic increase factor.

## INTRODUCTION

Progressive collapse is a catastrophic failure of a whole structure or a partial part of it that is caused by even a relative slightly initial local failure in structural element. Progressive collapse analysis attracts the attention of researchers such as the events of the Ronan Point and the 11 September 2001. Many researchers, therefore, started to focus on the causes of progressive collapse in building structures. To mitigate the potential for progressive collapse of building structures, many design codes such as DoD (2010) and GSA (2003) have been introduced. In recent studies, there are also many experimental and analytical studies conducted on the progressive collapse behaviors of buildings under the removing column scenarios. Alternative path loading method (APM) is proposed in such guidelines, which is not considering the type of the triggering event; rather, it considers the structural responses of the building. Such approach is also proposed by the design guidance of China CECS 392 (2014).

The steel-moment frame structure is one of the most commonly used structural systems. The structural performance to resist progressive collapse for steel frame structures attracts attention from many researchers. Recently, there are some experimental and analytical investigations on the progressive collapse behavior of composite steel frames under the missing column scenarios (Kim et al., 2009 & Feng, 2010 & Song et al., 2013). The progressive collapse mechanism analysis of the steel frame, cold-formed steel-framed, and bridge structures was also investigated by researchers (Ye et al., 2017 & Ye et al., 2018 & Jiang et al., 2018, & Jiang et al., 2019a & Jiang et al., 2019b & Jiang et al., 2020). Furthermore, a number of constructional technologies in improving the performance of the beam-column joints (Yang et al., 2013 & Liu et al., 2015) and floor slab (Kim et al., 2015) were proposed. It was found that the extreme rotation angle was the most important aspect to enhance the resistance of steel frames against progressive collapse. Furthermore, many researches found that not only the progressive collapse resistance of steel frame can be enhanced but also the dynamic responses can be reduced by adding trusses, braces, walls, etc. (Tsai et al., 2012). Zoghi et al. (2016) investigated the effect of infill steel panels on enhancing the progressive collapse resistance of moment frame structures. The effect of inverted-V bracing on retrofitting and strengthening the progressive collapse capacity of the steel moment frames was investigated by Rezvani et al. (2017). It was found that the inverted-V braces could enhance the resistance of the structure significantly except the cases for longer span and fewer number of stories. Salmasi et al. (2017) investigated the effect of inverted eccentrically V-shape and X-shape braces on progressive collapse-resisting capacity of steel moment frames, and the eccentrically inverted V-shape bracing system was found to exhibit more ductile behavior and better performance. However, there are a few studies focusing on the effects on layout types of such adding components in progressive collapse analysis.

Besides, the dynamic increase factor (DIF) is one of the most important parameters for the progressive collapse design of the building structures. Stevens et al. (2008) proposed an empirical DIF formula for steel structures, whose equation depended only on the parameter of the plastic rotation divided by yield rotation. Liu (2013) suggested a new DIF for nonlinear static progressive collapse analysis of building frames. Such new DIF considered the special level of gravity loads, and an empirical formula for the DIF was provided. Recently, Mashhadi et al. (2017) proposed a modified equation for DIF by considering the effects of moment demand, ductility, and postelastic stiffness ratio. However, such formulas were derived for the bare steel moment frame structures, and sole studies were conducted to analyze the effect of additional components on DIF of the steel moment frames.

Therefore, this paper investigates the progressive collapse resistance of the braced composite frames with different layout types of cross braces and column-removed scenarios by using the APM. The dynamic behavior of three 12-story composite steel frames with sudden loss of corner, side, and internal column is investigated. The vibration characteristics of the time-history curves were also analyzed. The comparison on dynamic increase factor for different layout types of braced frames is analyzed and discussed.

## CASE BUILDINGS

A typical 12-story steel-moment frame is selected as a benchmark structure. The height of the first story is 6.0 m, and it is 3.0 m for other stories. The steel frame is designed according to Chinese Standard GB 50009-2012 for gravity loads and GB 50011-2010 for seismic loads. A bare steel-moment frame (SF), a steel frame with braces installed in the middle bay (SF-VB), and a steel frame with braces installed in the highest story (SF-TB) are designed, and the planer layout of these frames is shown in Fig. 1. The steel columns are designed as box section with a size of 500×500×18×18 (500 mm and 18 mm are the side length and thickness, respectively). The steel beams are I section with a size of 450×200×9×14 (section height × flange width × web thickness × flange thickness). The steel cross braces are designed as I section with a size of 400×150×8×13. The reinforce concrete (RC) floors are designed with 150mm in thickness. All the steel components are Q345B grade, and the concrete is C30 grade.

The gravity loads including dead and live loads are obtained by the Chinese Standard GB50010 (2012), and they are 4.0kN/m$^2$ and 2.0kN/m$^2$, respectively. The dead and live loads of the roof are 4.0kN/m$^2$ and 0.5kN/m$^2$, respectively.

The wind load of these buildings is 0.5kN/m². The load combination function of this paper for dynamic analysis is determined according to the UFC code:

$$P = 1.2DL + 0.5LL + 0.2WL \tag{1}$$

where *DL*, *LL* and *WL* represent the dead load, live load, and wind load, respectively.
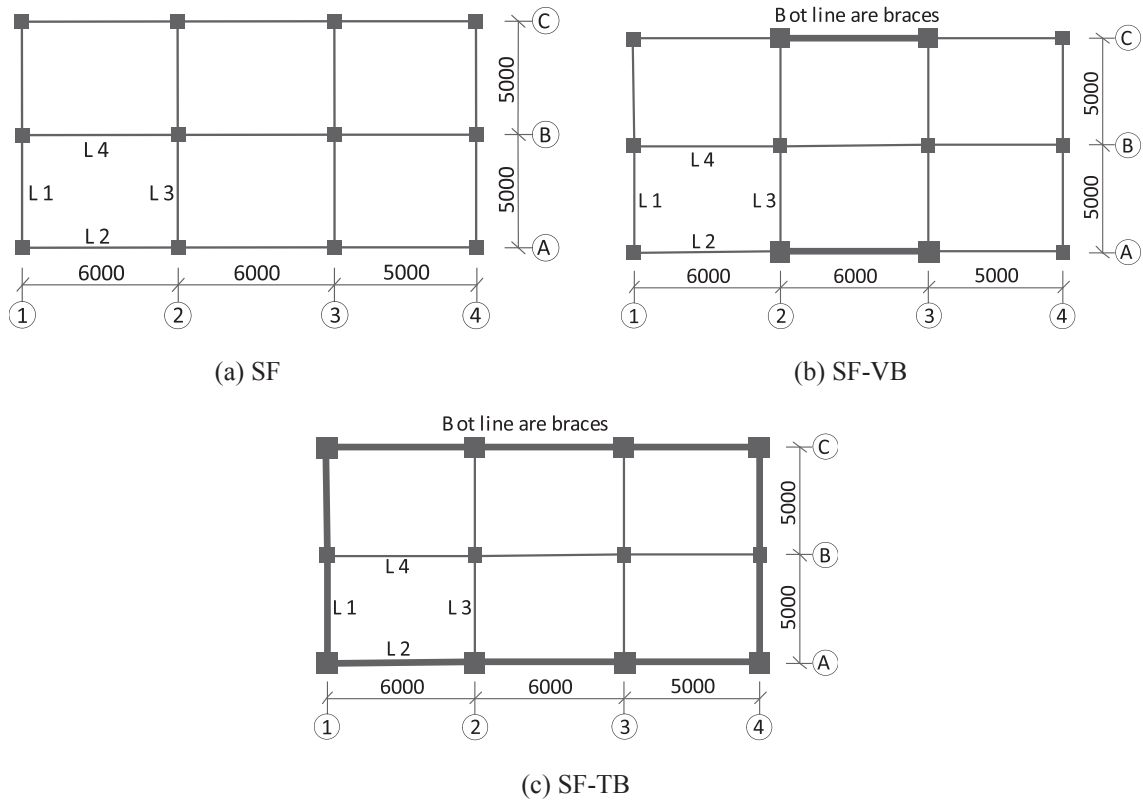
(a) SF

(b) SF-VB

(c) SF-TB

**Fig. 1.** Planar layout of the structures.

## NUMERICAL MODEL AND TEST VALIDATION

The numerical models of these buildings are established by the finite element software ANSYS, and they are shown in Fig. 2. The Beam 189 element is used to model the nonlinear behavior of the steel columns and beams, and the Shell 181 element is used to model the RC composite floor with profiled steel sheet. The profiled steel sheet is equivalent by bending stiffness, and the different material properties of steel and concrete are considered by "multi-layer shell" modelling method. The reinforcements in the composite floor are modeled by defining the area of reinforcement at the edge of the elements using the Link 180 element. The meshing size of all components of the steel frame was 50 mm, and the steel frame model was meshed 7372 elements and with 8084 nodes. Both the column bases and beam-column joints are considered as rigid connection. The connection between cross braces and beam-column joints is considered as pinned connection; the X-, Y, and Z axial directions are coupled for these connections in the FEM model.
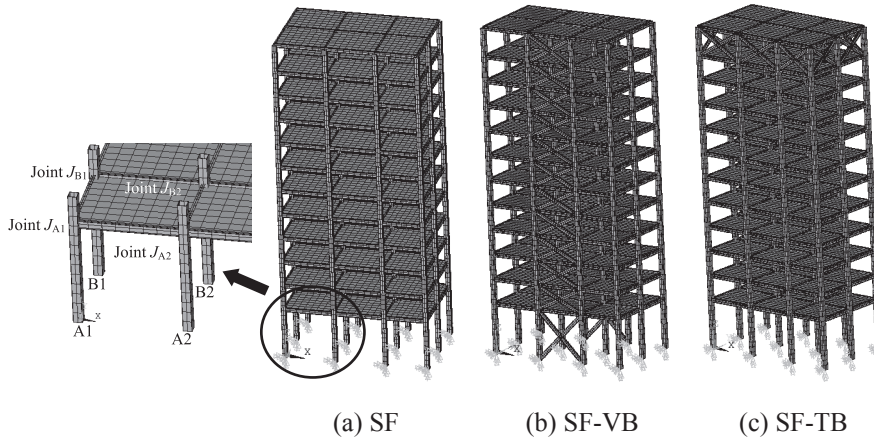
**Fig. 2.** FEM models for these 12-story frames.

## MATERIAL PROPERTIES

An idealized linear-plastic material model is used to model both the steel members and reinforcements; the yield strength and the elastic modulus of the steel are $f_y$=345MP and $E$=2.06×10$^5$ MPa, respectively. The Poison' ratio of the steel is determined as 0.3. A concrete damage plasticity model from ANSYS is utilized to model the nonlinear behavior of the concrete. The concrete is designed with 14.3 MPa in compressive strength and 1.43 MPa in tensile strength. The detailed strain-stress curve of the concrete is calculated by the Chinese Code GB 50010-2012, and the degradation part is determined according to the method presented by Hognestad model:

$$\sigma_c = f_c[1-(1-\frac{\varepsilon_c}{\varepsilon_0})^n] \qquad \text{if} \quad \varepsilon_c \leq \varepsilon_0 \qquad\qquad (2)$$

$$\sigma_c = f_c[1-0.15(\frac{\varepsilon_c - \varepsilon_0}{\varepsilon_{cu} - \varepsilon_0})^n] \qquad \text{if} \quad \varepsilon_0 < \varepsilon_c \leq \varepsilon_{cu} \qquad\qquad (3)$$

where the constant parameter is $n$=2, the $\varepsilon_0$=0.002, $\varepsilon_{cu}$=0.0033. The initial elastic modulus of the concrete is 3×10$^4$MPa, and the Poison' ratio is 0.2. The concrete is designed with 14.3 MPa in compressive strength and 1.43 MPa in tensile strength.

## TEST VALIDATION OF FEM

Progressive collapse test on a 4-bay single-story plane composite frame of Guo et al. (2013) is used to validate the numerical model established by finite element method (FEM) in this paper. A concentrated load $P$ was applied at the top of the removed column (Fig. 3) to perform quasistatic pushdown test for the specimen. The Shell181 and Beam189 elements are used to model concrete floors and beams based on the software of ANSYS, respectively. A bilinear hardening material model was used in the numerical model; the elastic modulus and yield strength of steel material were obtained from the test (Guo et al., 2013). The elastic modulus, compressive strength, and tensile strength of the concrete material were also acquired from the test. The failure modes obtained from the test and numerical model were presented in Fig. 3.

Fig. 4 shows the load-displacement curves of the FEM and test. It can be seen that the failure mode obtained from FEM is similar to the test, and the load-displacement curve acquired from FEM is similar to the test in the elastic and elastic-plastic stages. It can be concluded that the numerical model established in this paper can effectively predict the nonlinear behavior of the composite frame.
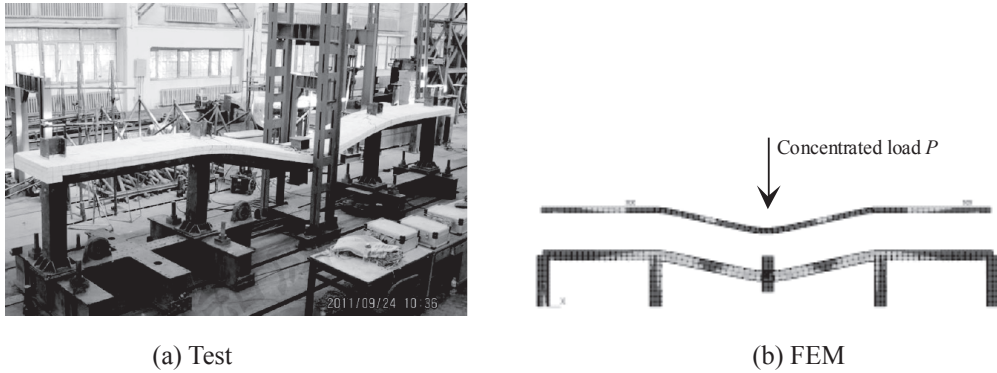
(a) Test                                                    (b) FEM

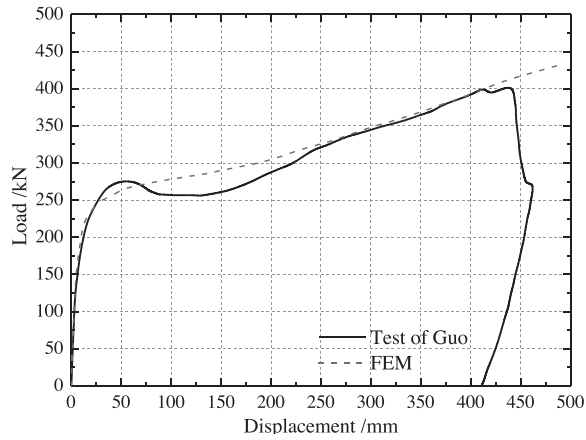**Fig. 3.** Failure modes of the frame (Guo et al. 2013).



**Fig. 4.** Load-displacement curve of FEM comparing with test.

## FREE VIBRATION ANALYSIS

To determine the vibration period of the residual structures, free vibration analyses are performed on these structures. The natural period $T_1$ as well as the period for vertical vibration mode $T_V$ is listed in Table 1.

**Table 1.** Natural vibration period of these structures.

| Model | Failure scenario | $T_1$ /s | $(T_1-T_0)$ /$T_0$ | $T_V$ /s |
|-------|------------------|----------|---------------------|----------|
| SF | A1 failed | 1.891 | 5.9% | 0.384 |
|    | A2 failed | 1.852 | 3.7% | 0.339 |
|    | B1 failed | 1.808 | 1.2% | 0.372 |
|    | B2 failed | 1.804 | 1.0% | 0.345 |
| SF-VB | A1 failed | 1.867 | 4.1% | 0.406 |
|       | A2 failed | 1.828 | 2.0% | 0.164 |
|       | B1 failed | 1.811 | 1.0% | 0.376 |
|       | B2 failed | 1.811 | 1.0% | 0.330 |
| SF-TB | A1 failed | 1.881 | 5.1% | 0.201 |
|       | A2 failed | 1.843 | 3.0% | 0.183 |
|       | B1 failed | 1.812 | 1.3% | 0.187 |
|       | B2 failed | 1.808 | 1.1% | 0.306 |

From Table 1, the top-layer braces decrease the period of the residual structures removing of A1, A2, and B1 columns in a larger margin. The vertical braces decrease the period of the residual structures removing from column A2, but the period is slightly increased for the other structures.

## ALTERNATIVE PATH METHOD (APM)

Four successive procedures are performed to evaluate the progressive collapse performance based on GSA guide: linear elastic static; nonlinear static; linear-elastic dynamic; and nonlinear dynamic. Among these four methods, the nonlinear dynamic method is proved to be the most thorough and accurate one. The nonlinear dynamic alternative path method (APM) is one of the most effective methods for progressive collapse analysis because the dynamic effect is considered in such method. The theoretical framework for APM is as follows: (1) a intact structure is allowed to reach its equilibrium under the applied loads; (2) then the target element is removed almost instantaneously, and the resulting motion of the residual structure is recorded; (3) lastly, the resulting deformations and forces of the residual structure are compared with the values of the intact structure, and dynamic increase factor is developed for progressive collapse design of the structure. Besides, such APMs have been adopted by the Department of Defense of the Unite States (DoD). In this study, the nonlinear dynamic analysis is adopted in the APM. In the numerical analysis, records of the vertical displacement of the joint at the top of the removed column were used to determine the dynamic behavior of the structures during the dynamic process. The failure time was determined as 0.5s according to the pretests and the performance of the computer. The column failed at the time of 0.1s, and it was deleted in the FEM analysis. The following section is the case studies for the events of A1-removed case, A2-removed case, B1-removed case, and B2-removed case. Rayleigh damping was used in the analyses. The Rayleigh damping factors were determined in the free vibration analyses.

$$[C] = \alpha[M] + \beta[K] \tag{4}$$

where $[C]$ is structural damping matrix; $[M]$ and $[K]$ are the mass and stiffness matrix, respectively; $\alpha$ and $\beta$ are the mass damping coefficient and the stiffness damping coefficient, respectively.

$$\alpha = \frac{2f_i f_j (\xi_i f_j - \xi_j f_i)}{f_j^2 - f_i^2}; \ \ \beta = \frac{2(\xi_j f_j - \xi_i f_i)}{f_j^2 - f_i^2} \tag{5}$$

where $f_i$ and $f_j$ are the $i$th and $j$th natural frequencies of the residual structure. $\xi_i$ and $\xi_j$ are damping ratios of the $i$th and $j$th vibration modes; this paper determines the damping ratio as 0.05 and selects the first-order and second-order vibration modes as the corresponding modes.

## RESULTS

Fig. 5 shows the effects of layout of cross braces on the dynamic time-history curves of the steel frame under different unforeseen events. The distribution of the plastic hinges of the residual structures subjected to A1 column-removed scenario is shown in Fig. 6.

(1) According to Fig. 5(a) and Fig. 5(c), the VB can not reduce the dynamic effect of the residual structure for the sudden failure of the column A1; on the contrary it may intensify the vertical dynamic vibration of the residual structure; the vertical displacement is intensified about 30%. The reason is that the VB enhances the lateral stiffness of the residual structures; thus the residual structures can not vibrate laterally to absorb the energy derived by the dynamic vibration of the floors in the column-removed bay. Therefore, the other bays of the residual structure would be protected by the VB for its effect on the prevention on progressive collapse developing in these bays. However, the dynamic behavior of the floors in column-removed bay would be intensified for all energy that should be absorbed by these floors.

(2) From the Fig. 5(b), the VB can mitigate the dynamic behavior of the residual structure for the VB-placed column-removed scenario. Because the VB provides new loading transmission paths for the residual structure, the maximum vertical displacement of the residual structure decreases from 19.2 mm to 13.1 mm for the A2 column-removed scenario.

(3) As shown in Fig. 5(a) - (c), the TB enhances the vertical stiffness of the structure; thus it can be used to reduce the dynamic effect of the residual structures for the corner column-removed and side column-removed scenarios, and the reduction is 30%-50%. Such reduction is more obviously observed for the A1 column-removed scenario. By comparing with the results for the A2 column-removed scenario, the maximum vertical displacement for the SF-TB is approximate with the value for the SF-VB. However, the vibration pattern of the time-history curve is unstable for the SF-TB subjected to A2 column-removed scenario. The reason is that the TB enhances the vertical stiffness of the top layer for the structure to a relatively great degree; thus a higher-order vibration model might occur in the residual structure for the difference in vertical stiffness between the top layer and the other layers. Therefore, instable vibration behavior is observed in the time-history curve for the SF-TB.

(4) Both VB and TB exhibit a very small impact on the time-history curves for the B2 column-removed scenario, as shown in Fig. 5(d). It can be concluded that the cross braces can only reduce the dynamic behavior of the residual structure for the column-removed scenario occurring in the brace placed bay. In fact, the DoD guidance also proposed the different dynamic increasing regions for the building structures according to the location of the removed column.
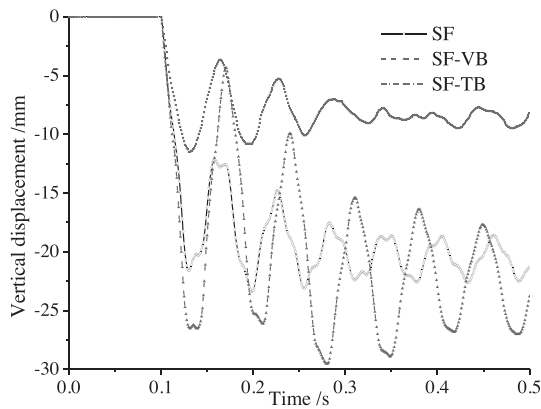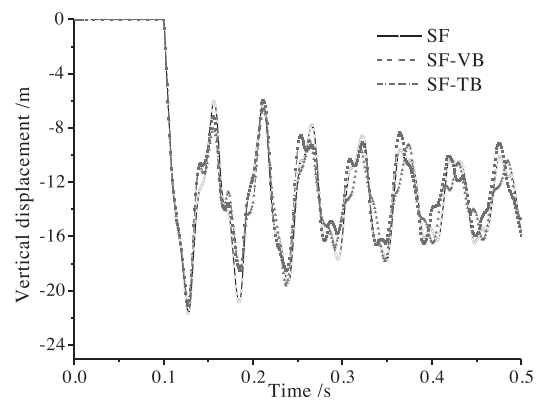


(a) Failure of column A1
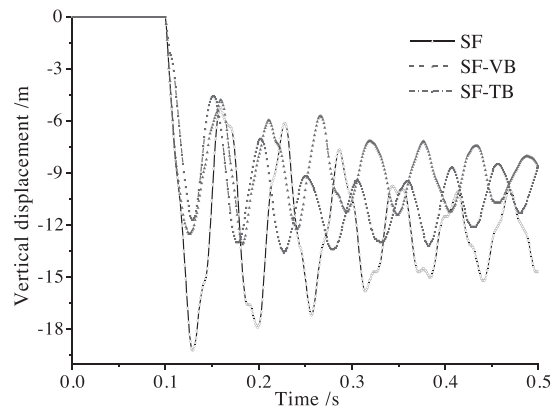
(b) Failure of column A2
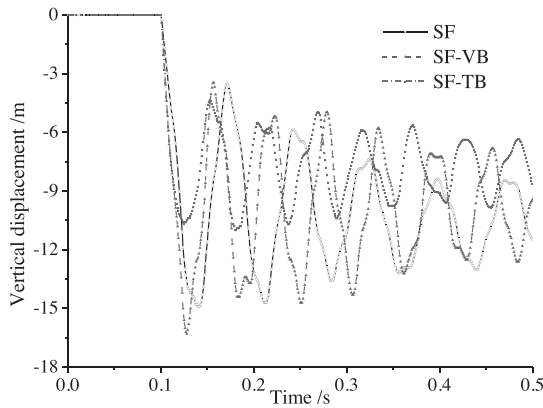
(c) Failure of column B1

(d) Failure of column B2

**Fig. 5.** Influence on displacement-time curves of the frame with cross braces.

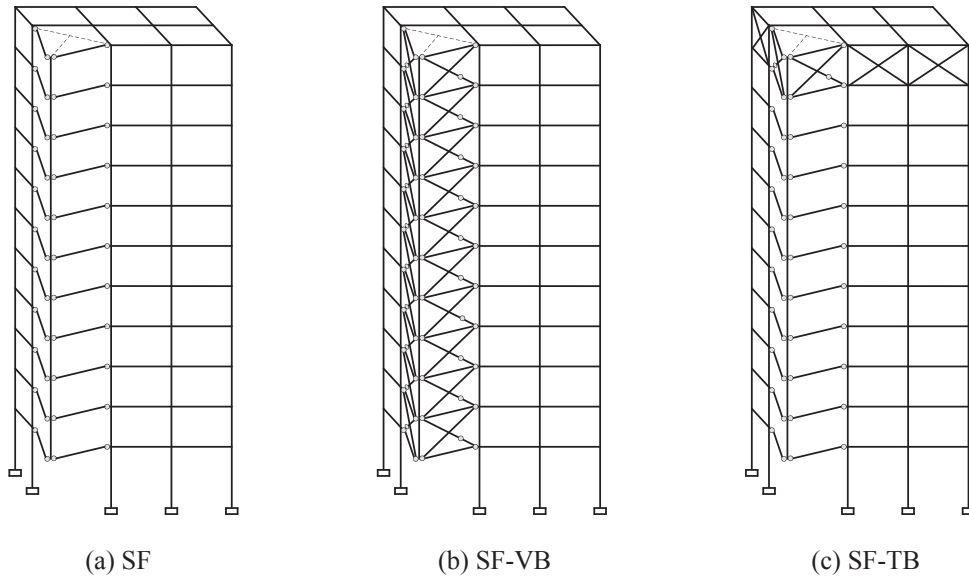|        (a) SF        |       (b) SF-VB       |       (c) SF-TB       |

**Fig. 6.** Plastic hinge distribution for the residual structure subjected to A1 column-removed scenario.

For the bare steel frame, the maximum vertical displacement is 23.4 mm for the column A1 removed scenario, with the displacement stabilizing at about 21 mm finally, because the composite floors and the frame beams start to support the additional dynamic loads for the sudden failure of the column A1, and the composite floor steps into nonlinear work stage. Regular attenuate vibration and obviously jumping phenomenon are observed in the curve. However, regular attenuate vibration phenomenon is found in the time-history curves of the A2, B1, and B2 column-removed scenarios. The vertical displacement of the residual structure is the minimal one for the B1 column-removed scenario, because the moment of the frame beam for B1 column-removed scenario is lower than the values for the other scenarios. The maximum vertical displacement of the residual structure for B2 column-removed scenario is slightly larger than the value for A2 column-removed scenario. Because the loading action region of the structure for B2 column-removed scenario is larger than the region for A2 column-removed scenario. The order of the maximum vertical displacement of the residual structures for these scenarios is A1-removed scenario > B2-removed scenario > A2-removed scenario > B1-removed scenario.

For the time-history curves for steel frame with VB, the residual structure exhibits maximum vertical displacement for the A1 column-removed scenario. The time-history curve of such residual structure presents two-step vibration and obviously jumping phenomenon is observed at about 0.25s. However, relatively regular attenuate vibration phenomenon is found in the time-history curves for the other column-removed scenarios. In general, the order of the maximum vertical displacement of the residual structures for these scenarios is A1-removed scenario > B2-removed scenario > A2-removed scenario > B1-removed scenario, which is the same with the bare steel frame.

According to the results of steel frame with TB, the residual structure corresponding to the B2 column-removed scenario exhibits maximum vertical displacement. The residual structures present regular attenuate vibration phenomenon in time-history curves for the B1 and B2 column-removed scenarios. The order of the maximum vertical displacement of the residual structures for these scenarios is B2-removed scenario > A2-removed scenario > A1-removed scenario > B1-removed scenario, whose order is different from the order of the bare steel frame and SF-VB.

The axial compression brace buckled and plastic hinge was formed at the center of the brace. The other brace sustained tension forces derived by the dynamic behavior of the residual structure. It can be found that the cross braces acted as vertical resisting components to mitigate the vertical dynamic affection. Thus the cross braces can be considered as the first defense line to resist the progressive collapse of the residual structures.

From Fig. 7 to Fig. 10, the axial force versus time-history curves for the columns corresponding to the different column-removed scenarios are shown.

(1) As the A1 column-removed scenario shown in Fig. 7, columns A2, B1, and B2 are affected by the dynamic behavior caused by the sudden failure of the column A1. It can be found that both VB and TB have shown small impact for column A2; however, the VB and TB increase the maximum axial force of columns B1 and B2, respectively.

(2) According to Fig. 8, for the A2 column-removed scenario, the maximum axial force of columns A1, B1, and B2 is affected slightly by the VB and TB. However, both the VB and TB have changed the shape of these curves, and the vibration amplitude of the axial force for the columns B1 and B2 is intensified by the VB.

(3) For the results of B1 column-removed scenario (Fig. 9), the maximum axial force of the columns A2 and B2 is reduced in a larger margin by both TB and VB, and the reduction is more obvious for the affection by the TB. However, both TB and VB increased the axial force of the column A1.

(4) As the results shown in Fig. 10, the maximum axial force of columns A2 and B1 is nearly unchanged by placing the VB and TB. However, such value is increased for column A1 by the effect of the VB.
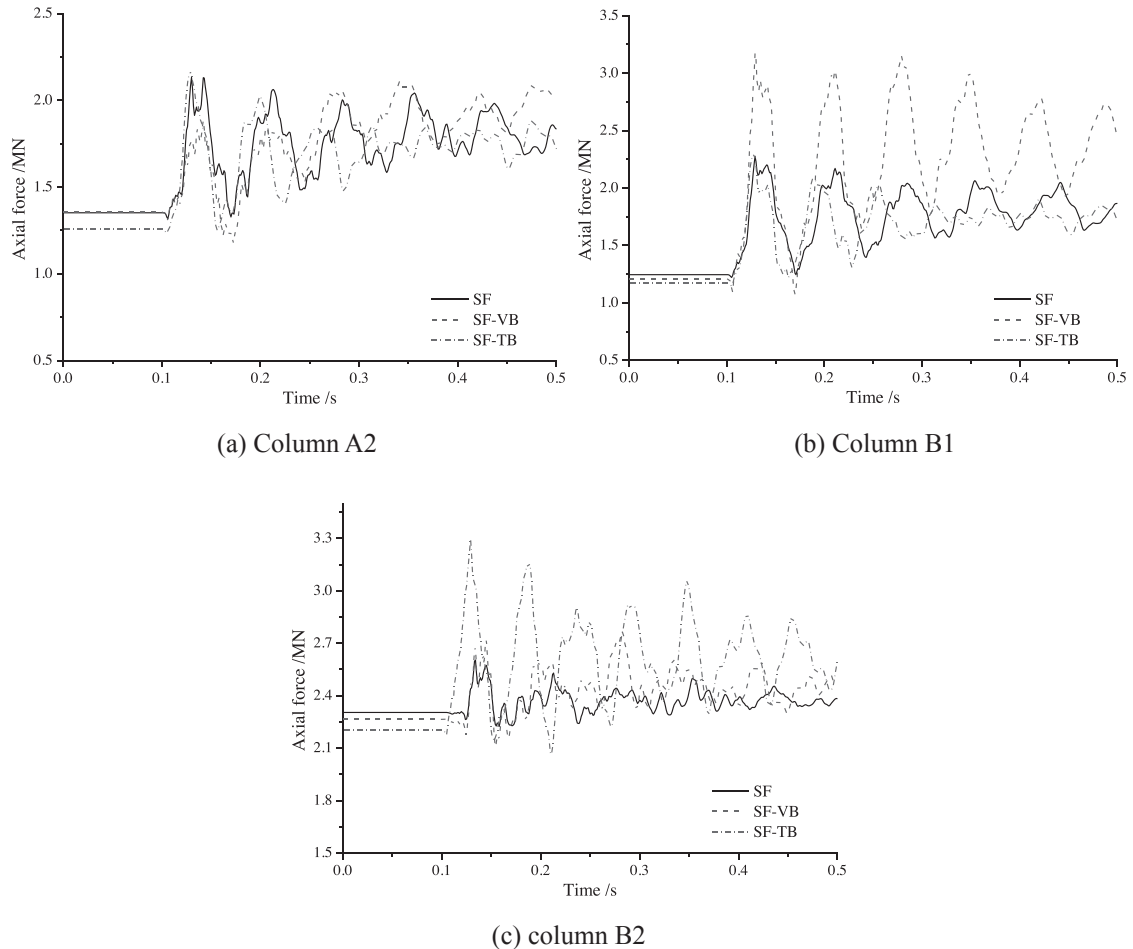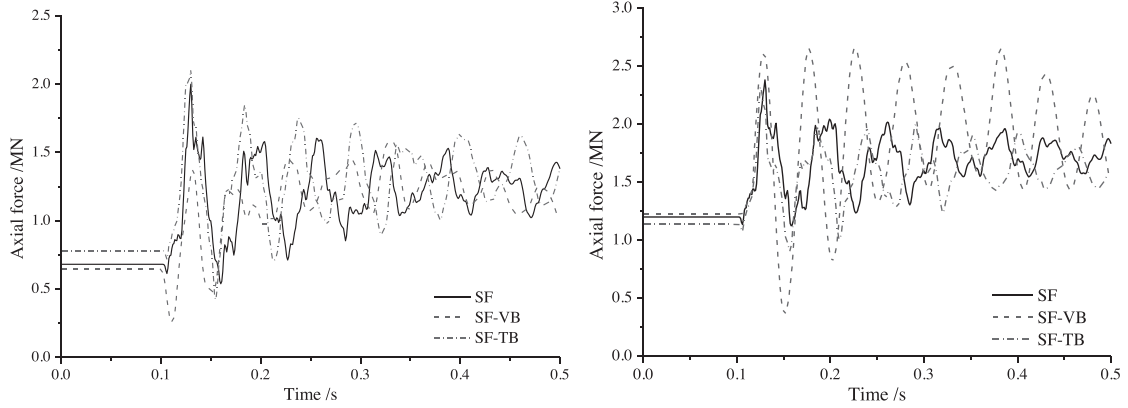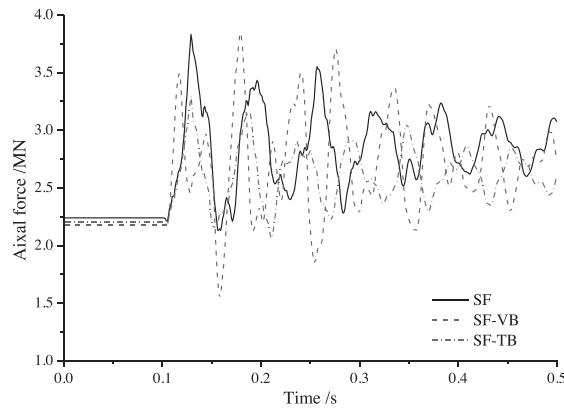


(a) Column A2

(b) Column B1

(c) column B2

**Fig. 7.** Axial-force versus time history curves for the A1 column-removed scenario.
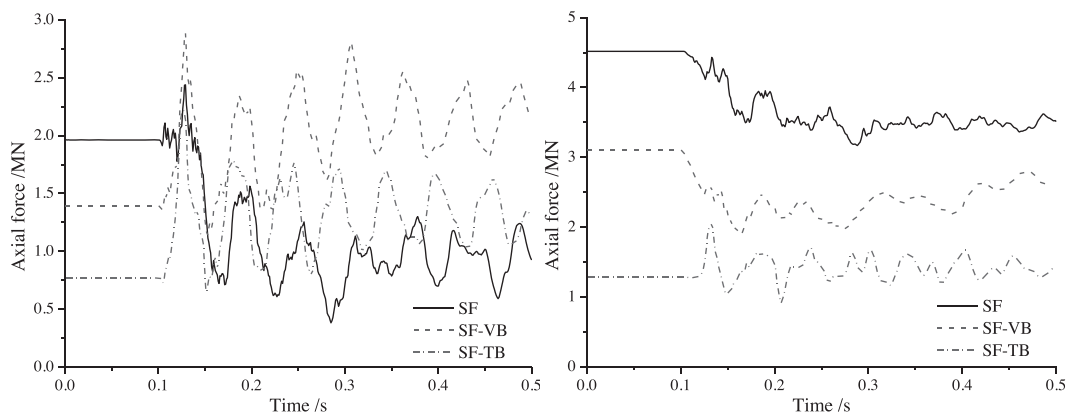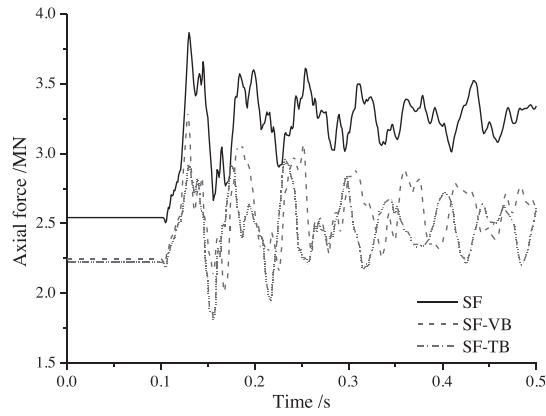
(a) Column A1

(b) Column B1



(c) column B2

**Fig. 8.** Axial-force versus time history curves for the A2 column-removed scenario.
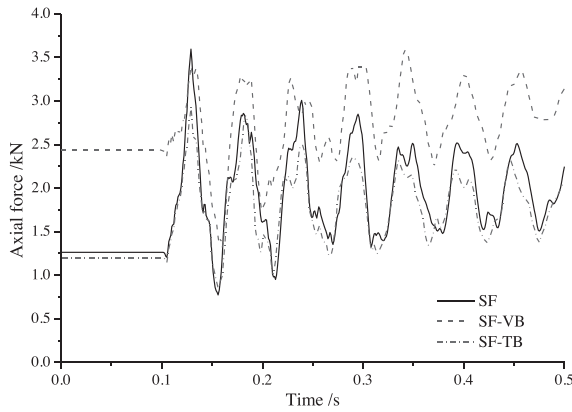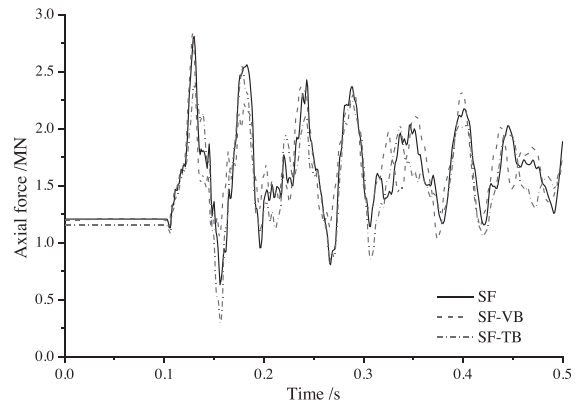


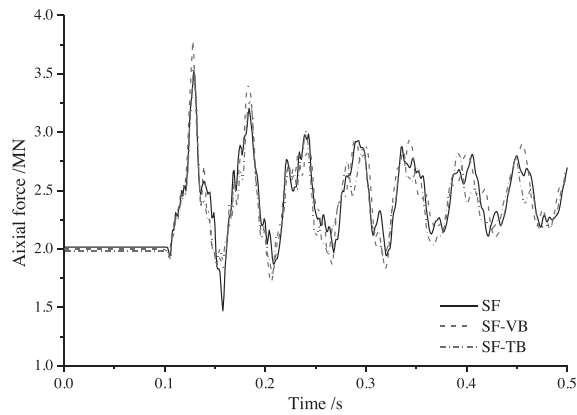(a) Column A1

(b) Column A2

(c) column B2

**Fig. 9.** Axial-force versus time history curves for the B1 column-removed scenario.



(a) Column A1



(b) Column A2



(c) column B1

**Fig. 10.** Axial-force versus time history curves for the B2 column-removed scenario.

Table 2 shows the dynamic increase factor (DIF) of the analyzed structures due to the different unforeseen events. It can be found that most of the DIF values are about 1.5 for the bare steel frame. However, the DoD guidance suggested that such value should be determined as 2.0. Indicating that the DIF values are conservative for the guidance, and such finding is similar with the findings from Steven et al. (2011) and Ruth et al. (2006).

It also can be found that both VB and TB affect the DIF of the structures in certain extent. For the A1 column-removed scenario, the TB reduces the DIF of the structure, but the VB intensifies such value; for the A2 column-removed scenario, the TB shows slightly impaction on DIF of the structure, but the VB reduces the DIF; for the B1 column-removed scenario, the TB has no influence on the DIF of the structure, but the TB increases such value; for the B2 column-removed scenario, both TB and VB have no influence on the DIF of the structures.

**Table 2.** Dynamic increase factor of the structures to unforeseen events.

| Failure scenario | SF | | | SF-VB | | | SF-TB | | |
|---|---|---|---|---|---|---|---|---|---|
| | $u_S$/mm | $u_D$/mm | $\beta_{SF}$ | $u_S$/mm | $u_D$/mm | $\beta_{SF-VB}$ | $u_S$/mm | $u_D$/mm | $\beta_{SF-TB}$ |
| A1 failed | 14.59 | 23.4 | 1.60 | 15.02 | 29.5 | 1.96 | 8.25 | 11.5 | 1.39 |
| A2 failed | 12.75 | 19.2 | 1.51 | 9.35 | 13.1 | 1.40 | 9.05 | 13.6 | 1.50 |
| B1 failed | 10.84 | 14.9 | 1.37 | 10.28 | 16.3 | 1.59 | 7.96 | 11.0 | 1.38 |
| B2 failed | 13.98 | 21.7 | 1.55 | 13.14 | 20.9 | 1.59 | 13.78 | 21.1 | 1.53 |

Note: $u_S$ is the vertical displacement of the target point subjected linear static load; $u_D$ is the maximum vertical displacement of the target point subjected nonlinear dynamic load; $\beta = u_D/u_S$ is the dynamic increase factor (DIF).

## CONCLUSIONS

This paper aims to investigate the influence on layout of cross braces for progressive collapse resistance of composite steel frame structures. The following conclusions are drawn:

1. The cross braces could enhance the progressive collapse resistance only for the scenario of the removed column, which is in the braces placed bay. But no obvious mitigation was observed in other bay. The VB obstructed the horizontal development of progress collapse of the buildings; thus it could be used to reduce the probability of progressive collapse developing in the other bay. However, the vertical braces aggravated the structural dynamic effects of the parts in the column-removed bay. The TB reduced the vertical displacement more than 50% caused by corner column-removed scenario; and the reduction was about 30% for the side column-removed scenario.

2. The dynamic increase factors (DIF) obtained from these cases were about 1.5, whose values were less than 2.0 defined in GSA and Chinese Standard, indicating that the DIF may be conservative defined in such Guidance. However, the DIF was closed to 2.0 for some column-removed scenarios for the building placed in VB, which should catch the engineers' attention.

3. To reduce the structural responses in progressive collapse analysis of the steel frames by adding cross braces, this paper suggests the following:

(1) For the corner column regions, the TB can be layout in the target bay to mitigate the negative influences caused by corner-removed scenario.

(2) To obstruct the horizontal development of progressive collapse of the structure, the VB can be placed in some required bays. Thus the structure would not be totally collapsed for some local damage.

(3) Such cross braces can be designed by also considering their contribution on seismic mitigation of the structures.

# ACKNOWLEDGMENT

# REFERENCES

**CECS 392. 2014.** Code for anti-collapse design of building structures. Beijing: China Planning Press.

**Department of Defense, DoD. 2010.** Design of structures to resist progressive collapse. Washington, D. C.

**Feng, F. 2010.** 3-D nonlinear dynamic progressive collapse analysis of multi-storey steel composite frame buildings- Parametric study. Engineering Structures, **32**(9): 3974-3980.

**GB 50009. 2012.** Load code for the design of building structures. Beijing: China Building Industry Press.

**General Services Administration, GSA. 2003.** Progressive collapse analysis and design guidelines for new federal office buildings and major modernization project. Washington, D. C.

**Guo, L.H., Gao, S., Fu, F. & Wang, Y. 2013.** Experimental study and numerical analysis of progressive collapse resistance of composite frames. Journal of Constructional Steel Research, **85**(9): 236-251.

**Jiang, L.Q. & Ye, J.H. 2018.** Risk-based robustness assessment of steel frame structures to unforeseen events. Civil Engineering and Environmental Systems, **35**(1-4), 117-138.

**Jiang, L.Q. & Ye, J.H. 2019a.** Collapse mechanism analysis of the FIU pedestrian bridge based on the improved structural vulnerability theory (ISVT). Engineering Failure Analysis, **104**: 1064-1075.

**Jiang, L.Q. & Ye, J.H. 2019b.** Redundancy of a mid-rise CFS composite shear wall building based on seismic response sensitivity analysis. Engineering Structures, **200**: 109647.

**Jiang, L.Q. & Ye, J.H. 2020.** Collapse mechanism and shaking table test validation of a 3D mid-rise CFS composite shear wall building. Thin-Walled Structures, **146**: 106470.

**Kim, J. & Kim, T. 2009.** Assessment of progressive collapse-resisting capacity of steel moment frames. Journal of Constructional Steel Research, **65**(1): 169-179.

**Kim, S., Lee, C.H. & Lee, K. 2015.** Effects of floor slab on progressive collapse resistance of steel moment frames. Journal of Performance of Constructed Facilities, **110**(2): 182-190.

**Liu, M. 2013.** A new dynamic increase factor for nonlinear static alternate path analysis of building frames against progressive collapse. Engineering Structures, **48**: 666-673.

**Liu, C., Fung, T. C. & Tan, K. H. 2015.** Dynamic Performance of Flush End-Plate Beam-Column Connections and Design Applications in Progressive Collapse. Journal of Structural Engineering, ASCE, 2015, 10.1061/ (ASCE)ST. 1943-541X. 0001329, 04015074.

**Mashhadi, J. & Saffari, H. 2017.** Modification of dynamic increase factor to assess progressive collapse potential of structures. Journal of Constructional Steel Research, **138**: 72-78.

**Rezvani, F.H., Taghizadeh, M.A.M. & Ronagh, H.R. 2017.** Effect of inverted-V bracing on retrofitting against progressive collapse of steel moment resisting frames. International Journal of Steel Structures, **17**(3). 1103-1113.

**Ruth, P., Marchand, K. A. & Williamson, E. B. 2006.** Static equivalency in progressive collapse alternate path analysis: reducing conservatism while retaining structure integrity. Journal of Performance of Constructed Facilities, **20**(4): 349-364.

**Salmasi, A.C. & Sheidaii, M.R. 2017.** Assessment of eccentrically braced frames strength against progressive collapse. International Journal of Steel Structures, **17**(2): 543-551.

**Song, B. & Sezen, H. 2013.** Experimental and analytical progressive collapse assessment of a steel frame building. Engineering Structures, **56**(5): 664-672.

**Stevens, D.J., Crowder, B., Hall, B. & Marchand, K. 2008.** Unified Progressive Collapse Design Requirements for DoD and GSA, Structures Congress, Vancouver Canada.

**Stevens, D., Crowder, B., Sunshine, D. & Waggoner M. 2011.** DoD research and criteria for the design of buildings to resist progressive collapse. Journal of Structural Engineering, **137**(9): 870-880.

**Tsai, M.H. 2012.** A performance-based design approach for retrofitting regular building frames with steel braces against sudden column loss. Journal of Constructional Steel Research,**77**(4): 1-11.

**Yang, B. & Tan, K.H. 2013.** Experimental tests of different types of bolted steel beam-column joints under a central-column removal scenario. Engineering Structures, **54**(9): 112-130.

**Ye, J.H., Jiang, L.Q. & Wang, X.X. 2017.** Seismic failure mechanism of reinforced cold-formed steel shear wall based on structural vulnerability analysis. Applied Sciences, **7**(2): 182-191.

**Ye, J.H. & Jiang, L.Q. 2018.** Collapse mechanism analysis of a steel moment frame based on structural vulnerability theory. Archives of Civil and Mechanical Engineering, **18**(3): 833-843.

**Zoghi, M.A. & Mirtaheria, M. 2016.** Progressive collapse analysis of steel building considering effects of infill panels. Structural Engineering and Mechanics, **59**(1): 59-82.